Environmental enrichment ameliorated high fat diet-induced Aβ deposition and memory deficit in APP transgenic mice.

Masato Maesako[1], Kengo Uemura[2], Masakazu Kubota[1], Akira Kuzuya[2], Kazuki Sasaki[1], Megumi Asada[1], Kiwamu Watanabe[2], Naoko Hayashida[1], Masafumi Ihara[2], Hidefumi Ito[2], Shun Shimohama[3], Takeshi Kihara[1] and Ayae Kinoshita[1*]

1. School of Human Health Sciences, Kyoto University Graduate School of Medicine, Kyoto 606-8507
2. Department of Neurology, Kyoto University Graduate School of Medicine, Kyoto 606-8507
3. Department of Neurology, Sapporo Medical University, Sapporo 060-8556

*Address correspondence to: Ayae Kinoshita,

School of Human Health Sciences, Kyoto University Graduate School of Medicine, 53, Shogoinkawahara-cho, Sakyo-ku, Kyoto 606-8507, Japan.

Tel. / Fax: 81-75-751-3969; E-mail: akinoshita@hs.med.kyoto-u.ac.jp

Abstract

The pathogenesis of Alzheimer's disease (AD) is tightly associated with metabolic dysfunctions. In particular, a potential link between type 2 diabetes (T2DM) and AD has been suggested epidemiologically, clinically and experimentally, and some studies have suggested that exercise or dietary intervention reduces risk of cognitive decline. However, there is little solid molecular evidence for the effective intervention of metabolic dysfunctions for prevention of AD. In the present study, we established the AD model mice with diabetic conditions through high fat diet (HFD) in order to examine the effect of environmental enrichment (EE) on HFD-induced AD pathophysiology. Here, we demonstrated that HFD markedly deteriorated memory impairment and increased β-amyloid (Aβ) oligomers as well as Aβ deposition in amyloid precursor protein (APP) transgenic mice, which was reversed by exposure to an enriched environment for 10 weeks, in spite of the continuation of HFD. These studies provide solid evidence that EE is a useful intervention to ameliorate behavioral changes and AD pathology in HFD-induced aggravation of AD symptoms in APP transgenic mice.

Keywords

Alzheimer's disease, type 2 diabetes, high fat diet, environmental enrichment, β-amyloid

The abbreviations

AD, Alzheimer's disease; T2DM, type 2 diabetes; HFD, high fat diet; Aβ, β-amyloid; APP, amyloid precursor protein; Tg, transgenic; WT, wild type; EE, environmental enrichment; IGTT, intra-peritoneal glucose tolerance test**;** CTF, C-terminal fragment

1. Introduction

Alzheimer's disease (AD), the most common cause of dementia, is poised to become a significant public health crisis. The occurrence of AD is largely sporadic, typically affecting individuals over 65 years, but a minority of the cases (5%) display familial inheritance with early onset. One of the pathological hallmarks of AD is amyloid plaques. Amyloid plaques are composed of 40–42 residue-peptides, called β-amyloid (Aβ) (designated as Aβ40, Aβ42), which are derived from the amyloid precursor protein (APP) via proteolytic cleavages by β- and

γ-secretases. Presenilin 1 and Presenilin 2 (PS1 and PS2) are known to be the catalytic core of γ-secretase (De Strooper *et al.* 1998). A widely accepted hypothesis about AD pathogenesis is that Aβ production plays a crucial role in neurodegeneration (Finder 2010). This hypothesis is supported by the discovery of causative mutations in the genes encoding APP, PS1, and PS2, in early onset familial AD (Tandon *et al.* 2000, Bertram *et al.* 2008). Moreover, recent studies have implied small soluble Aβ oligomers, such as dimers, trimers, and dodecamers, formed during Aβ aggregation, as being the main culprits of Aβ toxicity and AD pathogenesis (Hartley *et al.* 1999, Walsh *et al*. 2002, Lesne *et al*. 2006, Shankar *et al.* 2008).

A potential link between type 2 diabetes (T2DM) and AD has been suggested by epidemiological and clinical studies (Ott *et al.* 1999, Biessels *et al.* 2006). Recent experimental studies support this linkage. For example, APP-ob/ob mice, produced by crossing APP transgenic (Tg) mice with diabetic model mice, manifested earlier onset of cognitive dysfunction than APP Tg mice (Takeda *et al.* 2010). Moreover, using dietary interventions such as high fat diet (HFD) or sucrose water for APP Tg mice exacerbated their memory deficits and pathological alterations in the brain (Ho *et al.* 2004, Cao *et al.* 2007). On the other hand, insulin and the insulin-sensitizing drug have been shown to improve cognitive performance in mouse models of AD, as well as in patients with early AD (Watson *et al.* 2005, Pedersen *et al.* 2006, Reger *et al.* 2008). These reports clearly indicate that there is an association of diabetes with a higher risk of sporadic AD. However, the impact of non-pharmacological or preventive intervention targeting AD with diabetes has not been clearly demonstrated so far.

Exercise is beneficial in the prevention and treatment of T2DM, both in human and rodent models (Keller *et al.* 1993, Cotman and Berchtold 2007, Sanz *et al.* 2010). In the environmental enrichment (EE) condition, mice are allowed the freedom to move and exercise voluntarily in the larger cage, with accessibility to complex stimuli (e.g., toys, running wheels), thus being provided with more physical and intellectual stimulation than mice housed in standard laboratory conditions. In the AD research fields, some reports demonstrated that EE applied to AD model mice reduced Aβ deposition, enhanced synaptic plasticity, and ameliorated cognitive deficits (Lazarov *et al.* 2005, Jankowsky *et al.* 2005, Hu *et al.* 2010). On the other hand, other studies suggested that EE enhanced Aβ accumulation and failed to improve memory deficits in APP Tg mice with a regular diet (Jankowsky *et al.* 2003, Cotel *et al.* 2010). Thus, the effect of EE on AD pathophysiology has been controversial.

In the present study, in order to determine whether regular exercise affects cognitive decline, we established the AD model mice with diabetic conditions through HFD (APP-HFD mice), which were subsequently subjected to EE. To test the effect of EE, we conducted ethological, histochemical and biochemical analyses. Here, with the use of established animal models with both conditions, we observed that the APP-HFD mice exhibited even more impaired cognitive function than control APP Tg mice fed with normal diet (control APP mice). Additionally, we demonstrated that EE not only ameliorated obesity and glucose intolerance of the APP-HFD mice but also significantly improved their cognitive function. Notably, histochemical and biochemical analyses suggested that EE ameliorated the Aβ accumulation in the brains accelerated by HFD. Also, the amount of Aβ oligomers was elevated in the cerebrum of the APP-HFD mice, which was significantly reduced by EE settings. These results clearly indicated that EE could be an effective way to ameliorate the AD progression caused by metabolic dysfunctions.

2. Material and methods

2.1. Animals and dietary conditions

We used human APP Tg mice overexpressing the familial AD-linked mutations bearing both Swedish (K670N/M671L) and Indiana (V717F) mutation (APP*Swe/Ind*) (Mucke *et al.* 2000), which have been imported from the Jackson Laboratory (USA). APP*Swe/Ind* mice were maintained as heterozygotes and male and female mice were housed separately. Age- and sex-matched (1:1, male: female) mice were exposed to either an established high fat diet (HFD) (caloric composition, 60% fat, 20% carbohydrate, and 20% protein, Research Diet, Inc., Canada) or a standard diet (10% fat, 70% carbohydrate, and 20% protein, Oriental Yeast Co., Ltd., Japan) for 20 weeks, from 2-3 to 7-8 months age. To examine the effect of environmental enrichment (EE) on APP Tg mice fed with HFD (APP-HFD mice), the cage of the mice was changed to a 2.4 times larger one equipped with a running wheel as well as objects like stands and toys after 10 weeks of HFD (APP-HFD + EE mice). The mice spent 10 weeks in the EE condition in the presence of HFD. After the dietary manipulation, metabolic changes in these mice were analyzed, followed by the assessment of memory function through the Morris water maze test, as described below. After the analysis of memory function, the brains were extracted and were cut sagitally into left and right hemispheres. The left hemisphere was fixed in 4% paraformaldehyde for histological analysis. After removing the olfactory

lobe and cerebellum, the right hemisphere was rapidly frozen in liquid nitrogen for biochemical analysis. All animal experiments were performed in compliance with the Guidelines for the Care and Use of Laboratory Animals of the Kyoto University.

2.2 Assessment of metabolic changes

To assess glucose intolerance in these mice, we assessed changes in circulating glucose levels, as a function of time in response to the intra-peritoneal glucose tolerance test (IGTT). Mice were given a single dose of intra-peritoneal injection of glucose (2 g/kg body weight) after 14 hours fasting, and blood was collected from the tail-vein periodically over 2 hours. Blood glucose content was measured by using LabAssay Glucose (Wako, Japan). Plasma insulin concentration was measured by ELISA kit specific to insulin (Morinaga Seikagaku, Japan). Plasma concentrations of total cholesterol, High density lipoprotein (HDL)-cholesterol and triglyceride were measured by using cholesterol E-Wako, HDL-cholesterol E-Wako and triglyceride E-Wako (Wako, Japan).

2.3 Morris water maze test

Behavioral test was performed with a modified version of the Morris water maze test in order to assess spatial navigation learning and memory retention, as previously reported (Fitz *et al.* 2010), with minor modifications. Initially, animals received a habituation trial during which the animals were allowed to explore the pool of water (diameter 120 cm, height 25 cm, temperature 21±°C) without the platform present.

Visual cue phase. Following habituation, visible platform training was performed to measure motivation of the mice to find a platform, visual acuity of the mice, and the ability of mice to use local cues. Briefly, distal cues were removed from around the pool, and the platform was labeled with a flag and placed 1 cm above the surface of the water in the center of a quadrant. Mice were placed in the maze and allowed to explore the maze for 60 sec, and if they reached the visible platform, they were allowed to remain there for 20 sec before being returned to their cages. If they did not find the platform within 60 sec, the experimenter led them to the platform and let them remain there for 20 sec. Animals were trained in groups of five, and training was completed once each animal received six trials. This training was performed for 1 day.

Acquisition phase. We measured the ability of mice to form a representation of the spatial relationship between a safe, but invisible (submerged 1 cm below the water level), platform (10 cm in diameter) and visual cues surrounding the maze. The platform was located in the center of one of the four quadrants, and several extramaze cues were distributed across the walls surrounding the pool. During the acquisition phase of training, each mouse received four daily hidden platform training trials with 10-12 min intervals for 5 consecutive days. Animals were allowed 60 sec to locate the platform and 20 sec to rest on it. Mice that failed to find the platform were led there by the experimenter and allowed to rest there for 20 sec.

Probe trial phase. 24 hours following the last acquisition trial, a single 60 sec probe trial was administered to assess spatial memory retention. For the probe trial, animals were returned to the pool without the platform present, and parameters were recorded to assess the ability of the mouse to remember the previous location of the platform.

Performance was recorded with an automated tracking system (TARGET series/2, Japan) during all phases of training. During the visual cue phase of training, speed and latency to the platform were used to compare the activity of the performance between each group. During the acquisition phase, acquisition time (latency to reach the platform) and path length (swum distance) were subsequently used to analyze and compare the performance between different treatment groups. The time to the platform quadrant, and the number of entries into the target quadrant were recorded and analyzed during the probe trials.

2.4 Immunoblotting and filter trap assay

For immunoblotting analysis, the brain was extracted and rapidly frozen using liquid nitrogen. The brain samples from the cerebrum of the male mice were extracted in Radio-Immunoprecipitation Assay (RIPA) buffer (50 mM Tris-HCl, 150 mM NaCl, 1% Triton X100, 1% NP-40, 0.5% Deoxycholate, 0.1% SDS, pH 8.0) with protease inhibitor cocktail (Roche, Switzerland) and sufficiently homogenized on ice. Then the samples were incubated for one night at 4ºC and centrifuged at 14,000 g for 20 min. The supernatants were directly used for Western blot analysis. The detailed protocol has been described previously (Maesako *et al.* 2011). Mouse monoclonal anti-Aβ (6E10), β-actin, and rabbit polyclonal anti-APP C-terminal antibodies were from SIGMA (USA).

Filter trap assay was conducted as described previously (Kitaguchi *et al.* 2009). Briefly, the protein concentration of the samples in Tris-buffered saline (TBS)-extracted fraction was measured and an equal

amount of protein was subjected to vacuum filtration through a 96-well dot blot apparatus (Bio-Rad Laboratories) containing 200 nm pore-sized nitrocellulose membrane. The resultant membrane was then incubated with primary Aβ oligomer antibody (A11, Invitrogen; diluted 1:1000) at 4°C overnight. The membrane was then blocked by TBS containing 4% skim milk, and incubated with HRP-linked anti-mouse IgG secondary antibody (GE Healthcare; diluted 1:2000) for 1 hour. The membrane was developed using the ECL Western Blotting Analysis System (GE Healthcare). Aβ 42 peptides (BACHEM) incubated for 60 min at 37ºC was used as a positive control (Maesako *et al.* 2010) and monomeric Aβ was used as a negative control.

2.5. Immunohistochemistry

The paraformaldehyde-fixed and paraffin-embedded tissue sections of male mice were incubated with anti-Aβ (6E10) antibody (1:1,000). The sections were then incubated with biotinylated anti-mouse IgG antibody (1:2,000; Vector Laboratories, USA), followed by the incubation with avidin peroxidase (ABC Elite kit; 1:4,000; Vector Laboratories). Subsequently, the labeling was visualized by incubation with 50 mM Tris-HCl buffer (pH 7.6) containing 0.02% 3,3-diaminobenzidine and 0.0045% hydrogen peroxide. All images were visually analyzed using a microscope, ECLIPSE 80i (Nikon Corporation, Japan). On the other hand, for the fluorescent analysis, the tissue sections were incubated with anti-Aβ (6E10) antibody, followed by incubation with Alexa Fluor 488 anti mouse IgG (Invitrogen, USA). All images were visually analyzed, using a laser confocal scanning microscope, FV10i-LIV (Olympus Corporation, Japan). The Aβ immunoreactivity was quantified with Image J. For each animal, the sections were captured in the cortex and the hippocampus. Captured images then were imported into Image J, and an intensity threshold level was set that allowed for discrimination between plaque and background labeling. The total number of Aβ plaque associated pixels (6E10 antibody positive pixels) was calculated in each section, and then the Aβ load was calculated.

2.6. Measurement of Aβ by ELISA

The levels of Aβ 40, Aβ 42, or Aβ oligomers were measured by Enzyme-Linked ImmunoSorbent Assay (ELISA) kits specific to Aβ 40, Aβ 42, or Aβ oligomers (82E1-specific) (IBL, Japan), according to the manufacturer's instructions. We used a standard format for measuring monomeric Aβ species with the use of C-terminal capturing antibodies and N-terminal or mid-region detecting antibodies. On the other

hand, in order to detect Aβ oligomer species, the same N-terminal antibody, 82E1 (to Aβ residues 1–16, Immuno-Biological Laboratories, Inc, Minnesota, USA), was used for both capture and detection. In order to prepare the samples, the brain samples from the cerebrum of the male mice were homogenized with TBS. The homogenate was centrifuged at 100,000 g for 1 hour, and the supernatant was collected as the TBS-extracted fraction. Seventy percent formic acid (FA) was added to the pellet, which was homogenized again. The homogenate was incubated for 1 hour at 4°C and then centrifuged at 100,000 g for 1 hour at 4°C. The resultant supernatant was collected as the FA-extracted fraction, which was neutralized with a 20-fold volume of 1 M Tris buffer (pH 11.0).

2.7. Statistical analysis

All values are given in means ± SE. Comparisons were performed using an unpaired Student's t-test. For comparison of multiparametric analysis, one-way factorial ANOVA, followed by the post hoc analysis by Fisher's PLSD was used. Statistical significance of differences between mean scores during acquisition phase of training in the Morris water maze test was assessed with two-way repeated-measures ANOVA (general linear model/RM-ANOVA) and Fisher's post hoc analysis for multiple comparisons. $p < 0.05$ was considered to indicate a significant difference.

3. Results

3.1. Environmental enrichment ameliorated HFD-induced metabolic dysfunctions

Recent literature has demonstrated that HFD disrupts the metabolic conditions of APP Tg mice (Ho *et al.* 2004). To determine the effect of EE on HFD-induced metabolic dysfunctions, the cage of APP-HFD mice was changed into a larger one with a running wheel and objects like stands and toys. The mice were then fed with HFD for subsequent 10 weeks (Fig. 1). T2DM is characterized by obesity, glucose intolerance, and hyperinsulinemia (Defronzo 2009). According to our metabolic analysis using weekly monitoring of body weight, an intraperitoneal glucose tolerance test (IGTT) and the ELISA of serum insulin, obesity, glucose intolerance, and hyperinsulinemia were observed in the APP-HFD mice. Thus, we conclude that the APP-HFD mice, which we generated, exhibited severe T2DM conditions.

Although the APP-HFD mice gained significantly more body weight than the control APP mice (standard diet), the APP-HFD with EE (APP-HFD+EE) mice gained less body weight than the APP-HFD mice after the transfer to the EE setting (Fig. 2A). In spite of being fed with HFD, the APP-HFD+EE mice maintained an even body weight for 10 weeks. Weekly monitoring of food intake showed that the amount of food intake by the APP-HFD+EE mice was larger than that of the APP-HFD mice (supplemental Fig. 1), which indicated that the EE-mediated attenuation of body weight was not caused by the reduction of food intake. Moreover, we monitored the number of running wheel rotation and estimated that the APP-HFD+EE mice ran 1040±49 m per day in the EE setting. The fasting glucose level of the APP-HFD mice was increased, compared with that of the control APP mice, whereas that of the APP-HFD+EE mice was significantly decreased, compared with that of the APP-HFD mice (Fig. 2B). Further, the IGTT results indicated that the impaired glucose tolerance response of the APP-HFD mice was improved in the APP-HFD+EE group (Fig. 2C). To examine whether EE could reverse or prevent glucose tolerance abnormality, we conducted IGTT at the time of the switch from the standard environment to enriched one (10 weeks after HFD introduction). The fasting glucose level and glucose tolerance of APP-HFD+EE mice were better than those of the APP mice at the time of the switch (supplemental Fig. 2). Therefore, EE could reverse glucose tolerance abnormality. The ELISA results indicated that the level of plasma insulin was significantly increased in the APP-HFD mice. However, in contrast to the glucose level, plasma insulin level tended to decrease to some extent, but was not significantly different between the APP-HFD and APP-HFD+EE mice (Fig. 2D).

Next, we conducted plasma lipid analyses. The level of plasma total cholesterol in the APP-HFD mice was significantly increased, compared with that of the control APP mice. On the other hand, the total cholesterol level of the APP-HFD+EE mice was not different from that of the APP-HFD mice (Fig. 3A). Similarly, the level of plasma HDL cholesterol in APP-HFD mice was significantly increased, compared with that in the control APP mice. The plasma HDL level of the APP-HFD+EE mice was comparable with that of the APP-HFD mice (Fig. 3B). On the contrary, the level of plasma triglycerides was not different among the three conditions (Fig. 3C). Taken together, these results indicated that HFD disrupted the metabolic conditions including body weight, glucose tolerance, plasma insulin, and cholesterols of APP Tg mice, among which EE ameliorated body weight and glucose tolerance.

3.2 Environmental enrichment improved HFD-induced memory deficit

Recent literature also demonstrated that HFD leads to the worsening of memory deficit in APP Tg mice (Ho *et al.* 2004). To determine the effect of EE on HFD-induced memory deficit, we conducted the Morris water maze test. In our study, we analyzed 7- to 8-month-old APP Tg mice since they present with visible Aβ plaques and cognitive impairment sufficient for quantitative evaluations (Mucke *et al.* 2000). Neither HFD nor HFD+EE increased mortality of the mice, nor did they affect the motivation during the visual cue phase of the test (data not shown). In addition, neither HFD nor HFD+EE affected the locomotor activity of the mice, as exemplified by swimming speed (supplemental Fig. 3). During the acquisition phase, the control APP mice showed a daily improvement in their performance, such as acquisition time (Fig. 4A) and path length to the platform (Fig. 4B), whereas the APP-HFD mice did not show any improvement. On the other hand, the APP-HFD+EE mice showed better performance than the APP-HFD mice did (Fig. 4A, B). Moreover, the probe trial demonstrated that the APP-HFD mice took a longer time to get to the platform quadrant (Fig. 4C) and failed to cross the previous location of the platform (Fig. 4D), compared to control mice. Once again, the APP-HFD+EE mice showed better performance than the APP-HFD mice, in this probe trial phase as well (Fig. 4C, D). From these results, we concluded that EE ameliorated HFD-induced memory dysfunction, despite continuing HFD in the AD model mice.

In order to determine whether these events were attributable to metabolic consequences of the diet or to an interaction between the diet and neuropathology in AD model mice, wild type (WT) mice were tested for learning ability, using the Morris water maze test. Metabolic analyses indicated that WT mice also exhibited T2DM conditions (supplemental Fig. 4A, B). After the 4^{th} day, in the acquisition phase of Morris water maze test, acquisition time of the HFD-induced WT (WT-HFD) mice was not different from that of the control WT or the WT-HFD+EE mice, although that of the WT-HFD mice was longer than that of the control WT and the WT-HFD+EE mice from 1^{st} to 3^{rd} day (supplemental Fig. 4C). This tendency was different from the case of the APP mice, since APP-HFD mice consistently took longer time to get to the platform quadrant in the acquisition phase (Fig. 4A). These results suggested that memory dysfunction could be attributable to an interaction between the diet and neuropathology in the AD model mice.

3.3 HFD-induced Aβ deposition was ameliorated in environmental enrichment condition

HFD is reported to lead to Aβ accumulation in the brain of APP Tg mice (Ho *et al.* 2004). We considered the possibility that the memory impairment in APP-HFD mice was due to ample Aβ deposition, and wanted to see the effect of environmental change on HFD-induced Aβ accumulation. Therefore, we conducted immunohistochemical analysis using anti-Aβ (6E10) antibody to quantitatively examine Aβ deposition. As seen in Figure 5A–C, Aβ deposition in the hippocampus was aggravated in the APP-HFD mice, whereas EE introduction resulted in a marked reduction of HFD-induced Aβ deposition in the APP-HFD+EE mice.

We next quantified Aβ contents in the TBS-soluble and -insoluble (FA soluble) fractions using ELISA. In the TBS-soluble fraction, the levels of Aβ 40, Aβ 42, and total Aβ in the APP-HFD mice were comparable to that in the control APP mice. However, the levels of Aβ 40 and total Aβ in the APP-HFD+EE mice were significantly decreased, compared with that in the APP-HFD mice (Fig. 5D–F). On the other hand, in FA fraction, the level of Aβ 40 in the APP-HFD mice was significantly increased, compared with that in the control APP mice. However, the levels of Aβ 40 in the APP-HFD+EE mice were significantly decreased, compared with that in the APP-HFD mice (supplemental Fig. 5A). A similar tendency was shown in the case of Aβ 42 and total Aβ amount in FA fraction, although there was no statistical significance (supplemental Fig. 5B, C). Based on these histochemical and biochemical analyses, we concluded that EE ameliorated HFD-induced Aβ accumulation in the brain.

Recent reports suggest that the level of soluble Aβ oligomers correlate with memory deficits in APP Tg mice (Hartley *et al.*1999, Walsh *et al*. 2002, Lesne *et al*. 2006, Shankar *et al.* 2009). To determine a correlation between Aβ oligomers and memory impairment in standard housing APP-HFD mice and APP-HFD+EE mice, we performed the ELISA analysis using Aβ oligomer-specific ELISA kit (Xia *et al.* 2009). The level of TBS-soluble Aβ oligomers in the APP-HFD mice was significantly increased, compared with that in the control APP mice. This result was consistent with that of the test for memory assessment described above. Remarkably, the levels of Aβ oligomers in the APP-HFD+EE mice were significantly decreased, compared with that in the APP-HFD mice (Fig. 5G). In addition, we confirmed this result through Filter trap assay, using anti-Aβ oligomer antibody (supplemental Fig. 6). Thus, at least in HFD-induced conditions, EE appears to play a significant role in modulating the level of Aβ oligomers.

3.4 Alteration of HFD-induced APP processing by environmental enrichment

To elucidate the mechanism of how EE ameliorated HFD-induced Aβ accumulation, we analyzed the APP processing through detecting APP C-terminal fragments (CTFs: CTFα, β) through immunoblotting assay. α- and β-Secretases are known to cleave APP at the extramembrane domain, which produce APP-CTFα and CTFβ respectively. γ-Secretase cleaves APP-CTFα and CTFβ at the intramembrane domain, producing p3 and Aβ respectively. As shown in the top row of Figure 6A, the level of full length APP was not different among the control, APP-HFD, and APP-HFD+EE mice (Fig. 6B). In this experiment, we used anti-APP C-terminal antibody to detect both APP-CTFα and CTFβ. Notably, APP CTFs were more accumulated in the brains of the APP-HFD mice than those of the control APP mice. However, the level of APP CTFs in the APP-HFD+EE mice was significantly decreased, compared with that in the APP-HFD mice in standard housing (Fig. 6C). Next, we examined the amount of APP-CTFβ by anti-Aβ (6E10) antibody which detects 1–17 amino acid residues of Aβ. The analysis using 6E10 antibody showed that the level of APP-CTFβ in the APP-HFD mice was higher than that in the control APP mice, suggesting that the level of APP-CTFβ in the APP-HFD+EE mice was significantly decreased, compared with that in the APP-HFD mice (Fig. 6D).

4. Discussion

HFD is prevalent in modern society and HFD-induced metabolic condition is becoming a worldwide issue, since it leads to obesity, T2DM, and hypercholesterolemia. More importantly, recent studies have shown that diet and nutrition have been recognized as important epigenetic factors for the development of sporadic AD (Solfrizzi *et al.* 2003, Panza *et al.* 2006, Scarmeas *et al.* 2007). We and others have previously proposed the causal molecular link between T2DM and AD (Qiu *et al.* 2006, Maesako *et al.* 2010, Maesako *et al.* 2011). However, the effective prevention for AD has not been fully investigated yet. A recent report by McClean *et al.* showed compelling evidence that the diabetes drug liraglutide prevents neuronal degeneration in a mouse model of AD (McClean *et al.* 2011), which suggests that there should be a clinical association of diabetic change with a higher risk of neuronal loss. This further led us to consider a development of an effective prevention in the early phase of AD. To address this issue, we established the AD model mice with diabetic conditions in the present study, by HFD feeding in APP Tg mice.

In order to search for an effective intervention, we chose a paradigm of environmental enrichment (EE) and

examined the effect of EE on both the metabolic conditions and the AD pathology of the mice (Fig. 1). A recent retrospective case control study demonstrated that AD patients were less active (both intellectually and physically) in midlife and that inactivity was associated with a 2.5 fold higher risk of developing AD (Friedland *et al.* 2001). Similarly, a prospective study revealed that physical activity was protective against the development of cognitive impairment in AD and that the highest activity group showed the incidence of AD lowered by 60% (Laurin *et al.* 2001). Since EE is regarded as a useful tool for exercise in mice, we chose this paradigm in the present study to see the impact of exercise on AD pathophysiology. Importantly, Adlard *et al.* have demonstrated that voluntary exercise shows beneficial effects on a Tg mice model of AD (Adlard *et al.* 2005). Since EE condition contains physical and intellectual stimulation, the extent to which intellectual stimulation contributes to the positive outcome still remains controversial. Faherty *et al.* suggested that EE is more effective for facilitating neural changes than exercise alone (Faherty *et al.* 2003), while Lambert *et al.* suggested that exercise, but not cognitive stimulation, improves spatial memory (Lambert *et al.* 2005). In the setting of the present study, metabolic conditions of the APP-HFD+EE mice were clearly ameliorated, compared to those of the APP-HFD mice. Moreover, cognitive stimulation of our setting was smaller than that in previous reports, since we wanted to focus on the effect of exercise on APP-HFD mice. Therefore, we speculated that physical stimulation might play a more important role in our study. The purpose of this experiment was to obtain a deep insight into developing strategies for the prevention of AD; therefore, EE was started at the age before the appearance of visible Aβ plaques in the brain of APP *Swe/Ind* mice.

Although previous reports examined the effect of EE on AD model mice (Jankowsky *et al.* 2003, Lazarov *et al.* 2005, Jankowsky *et al.* 2005, Hu *et al.* 2010, Cotel *et al.* 2010), the effect of EE on AD mice with diabetic conditions had not yet been examined. Notably, our results indicated that EE ameliorated HFD-induced memory deficit, in spite of continuing high-fat feeding (Fig. 4). EE is known to enhance hippocampal neurogenesis and result in increased numbers of synapses per neuron (Hu *et al.* 2010). We assumed that EE might have improved cognitive dysfunctions of the mice through strengthening of the synaptic activity of the mice. Further, our results demonstrated that EE decreased oligomers and fibrillar Aβ, indicating that EE also ameliorated HFD-induced Aβ accumulation (Fig. 5). An increasing number of reports have suggested that the level of soluble Aβ oligomers correlates with memory deficits due to their synaptotoxicity (Hartley *et al.* 1999, Walsh *et al*. 2002, Lesne *et al*. 2006, Shankar *et al.* 2009, Jin *et al.* 2011). Therefore, we hypothesized that

EE also might have improved memory deficit of the mice through the decrease of soluble Aβ oligomers, followed by the improvement of Aβ plaque depositions. Notably, Cotel *et al*. have reported that EE failed to rescue working memory deficits and neuronal loss in APP/PS1 knock-in (KI) mice (Cotel *et al*. 2010). Their result is different from ours in that enriched housing did not show any beneficial effects in terms of working memory and amyloid burden. Our result was obtained from high-fat feeding of APP Tg mice, whereas Cotel *et al*. used conventional diet for APP/PS1 KI mice; however, housing conditions seem similar. We suppose that the combination of physical activity and cognitive stimulus in EE condition may be more beneficial in the reversal of cognitive decline and Aβ load, which was caused by metabolic dysfunctions due to high-fat feeding.

To clarify the effect of EE on HFD-induced AD pathology, we first investigated the mechanisms of how HFD aggravated Aβ depositions. Recent literature has suggested that HFD down-regulates the activity of Insulin degrading enzyme (IDE), one of the Aβ degrading enzymes (Ho *et al.* 2004). In addition, we demonstrated that HFD increased the level of APP CTFβ without a change in full-length APP levels (Fig. 6). Unexpectedly, we could not detect the difference of BACE1/β-secretase level among control APP, APP-HFD, and APP-HFD+EE mice's brains (supplemental Fig. 7A, B). Although emerging evidence has consistently detected significant increases in β-secretase enzyme activity in the sporadic AD brains, the BACE1 enzyme activity in AD is not necessarily reflected by its protein levels (Stockley and Neill 2008), presumably because BACE1 enzyme activity might be regulated by other factors such as trafficking, and subcellular and membrane microdomain localization. Moreover, recent literature has demonstrated that BACE1 enzyme activity is modulated by sphingosine-1-phosphate (S1P), a pluripotent lipophilic mediator (Takasugi *et al.* 2011), suggesting that BACE1 interacting proteins can also control its activity. We compared the BACE1 interacting proteins of the APP-HFD mice brain samples with that of the control-APP samples by immunoprecipitation assay using BACE1 antibody and determined the different profiles in interacting proteins between them (unpublished observation). We speculate that HFD might have changed the interacting state of these proteins with BACE1, without changing the BACE1 protein level. Consequently, we conclude that HFD could have aggravated Aβ accumulation via several pathways, including the activation of BACE1/β-secretase enzyme and the inhibition of Aβ degradation.

Next, to reveal the mechanism of beneficial effect of EE, we employed ELISA experiments. The ELISA results in TBS-soluble fraction indicated that HFD might not simply increase the production of Aβ,

but that HFD affects the aggregation and deposition of Aβ (Fig. 5D-F). On the other hand, considering that EE decreased the level of APP CTFβ (Fig. 6), we assume that EE could have inhibited HFD-induced BACE1/β-secretase up-regulation. We speculate that EE could also have changed the state of interacting proteins with BACE1. However, EE also might have improved Aβ accumulation via the up-regulation of Aβ clearance, since EE activates Neprilysin, one of the Aβ degrading enzymes (Lazarov *et al.* 2005). Interestingly, our metabolic analyses suggested that EE did not affect either HFD-induced hyperinsulinemia or hypercholesterolemia, but improved body weight as well as glucose tolerance (Fig. 2, 3), indicating that EE might have ameliorated HFD-induced Aβ accumulation through the improvements in obesity and glucose tolerance. According to a recent review by Misra, the EE-mediated improvement of glucose tolerance via insulin independent pathway may be caused by the role of adenosine monophosphate (AMP)-activated protein kinase (AMPK) since it is considered a master switch to regulate glucose level without an effect on insulin in exercise-related effects (Misra 2008). To develop an effective intervention, it is important to elucidate the relationship between obesity and glucose intolerance and HFD-induced Aβ accumulation as well as memory deficit.

In conclusion, we provide convincing evidence that EE ameliorated HFD-induced metabolic dysfunctions, Aβ deposition, and memory deficit. We showed that EE improved metabolic conditions like obesity and glucose intolerance in APP-HFD mice without rectifying the level of serum insulin. Our result is clinically intriguing in that a rather mild intervention like EE for only 10 weeks prevented further HFD-induced cognitive decline in the AD mouse model. However, the detailed mechanism of how EE ameliorated HFD-induced Aβ deposition and memory deficit was not clarified in the present study. Although the exact pathogenesis of sporadic AD remains still largely unknown, our results clearly indicate that the intervention for the metabolic condition could be the most effective and practicable way to prevent AD in T2DM patients. Considering that the beneficial effect was obtained even with the continuation of HFD, the detailed mechanism of continuous exercise and its practical application to AD patients should be further verified in future studies.

5. Acknowledgement

We would like to give our thanks to Dr. S.Oka (Kyoto University, Kyoto, Japan), Mr. J.Morise (Kyoto University, Kyoto, Japan), Dr. Y. Kitamura (Kyoto Pharmaceutical University, Kyoto, Japan) and Dr. K. Takata (Kyoto Pharmaceutical University, Kyoto, Japan) for technical assistance of the brain sample preparation. We would like to give our thanks to Dr. K.Saito (Kyoto University, Kyoto, Japan) for kind support of the Morris water maze test. We greatly appreciate the advice for metabolic analysis to Dr. M. Okuda (PHARMAEIGHT. Kyoto, Japan). We would like to give our thanks to Dr. Y. Tashiro (Kyoto University, Kyoto, Japan) for kind discussion. The work was financially supported by Grant-in-Aid from the Ministry of Education, Culture, Sports, Science and Technology (20300124), the Research Grant from Takeda Science Foundation, the Research Grant from the Kanae Foundation for the Promotion of Medical Science and the Research Grant from the Nakatomi Foundation.

Disclosure statement: The authors declare that they have no actual or potential conflict of interest.

6. References

Adlard PA, Perreau VM, Pop V, Cotman CW. Voluntary exercise decreases amyloid load in a transgenic model of Alzheimer's disease. J Neurosci. 2005;25(17):4217-21.

Bertram L, Tanzi RE. Thirty years of Alzheimer's disease genetics: the implications of systematic meta-analyses. Nat Rev Neurosci 2008;9(10):768-78.

Biessels GJ, Staekenborg S, Brunner E, Brayne C, Scheltens P. Risk of dementia in diabetes mellitus: a systematic review. Lancet Neurol 2006;5(1):64-74.

Cao D, Lu H, Lewis TL, Li L. Intake of sucrose-sweetened water induces insulin resistance and exacerbates memory deficits and amyloidosis in a transgenic mouse model of Alzheimer disease. J Biol Chem 2007;282(50):36275-82.

Cotel MC, Jawhar S, Christensen DZ, Bayer TA, Wirths O. Environmental enrichment fails to rescue working memory deficits, neuron loss, and neurogenesis in APP/PS1KI mice. Neurobiol Aging. in press

Cotman CW, Berchtold NC. Physical activity and the maintenance of cognition: learning from animal models. Alzheimers Dement. 2007 ;3:S30-7.

De Strooper B, Saftig P, Craessaerts K, Vanderstichele H, Guhde G, Annaert W, Von Figura K, Van Leuven F. Deficiency of presenilin-1 inhibits the normal cleavage of amyloid precursor protein. Nature 1998;391(6665):387-90.

Defronzo RA. Banting Lecture. From the triumvirate to the ominous octet: a new paradigm for the treatment of type 2 diabetes mellitus. Diabetes 2009;58(4):773-95.

Faherty CJ, Kerley D, Smeyne RJ. A Golgi-Cox morphological analysis of neuronal changes induced by environmental enrichment. Brain Res Dev Brain Res. 2003;141(1-2):55-61.

Finder VH. Alzheimer's disease: a general introduction and pathomechanism. J Alzheimers Dis;22 Suppl 3:5-19.

Fitz NF, Cronican A, Pham T, Fogg A, Fauq AH, Chapman R, Lefterov I, Koldamova R. Liver X receptor agonist treatment ameliorates amyloid pathology and memory deficits caused by high-fat diet in APP23 mice. J Neurosci 2010;30(20):6862-72.

Friedland RP, Fritsch T, Smyth KA, Koss E, Lerner AJ, Chen CH, Petot GJ, Debanne SM. Patients with Alzheimer's disease have reduced activities in midlife compared with healthy control-group members. Proc Natl Acad Sci U S A 2001;98(6):3440-5.

Hartley DM, Walsh DM, Ye CP, Diehl T, Vasquez S, Vassilev PM, Teplow DB, Selkoe DJ. Protofibrillar intermediates of amyloid beta-protein induce acute electrophysiological changes and progressive neurotoxicity in cortical neurons. J Neurosci 1999;19(20):8876-84.

Ho L, Qin W, Pompl PN, Xiang Z, Wang J, Zhao Z, Peng Y, Cambareri G, Rocher A, Mobbs CV, Hof PR, Pasinetti GM. Diet-induced insulin resistance promotes amyloidosis in a transgenic mouse model of Alzheimer's disease. FASEB J 2004;18(7):902-4.

Hu YS, Xu P, Pigino G, Brady ST, Larson J, Lazarov O. Complex environment experience rescues impaired neurogenesis, enhances synaptic plasticity, and attenuates neuropathology in familial Alzheimer's disease-linked APPswe/PS1DeltaE9 mice. FASEB J 2010;24(6):1667-81.

Jankowsky JL, Melnikova T, Fadale DJ, Xu GM, Slunt HH, Gonzales V, Younkin LH, Younkin SG, Borchelt DR, Savonenko AV. Environmental enrichment mitigates cognitive deficits in a mouse model of Alzheimer's disease. J Neurosci 2005;25(21):5217-24.

Jankowsky JL, Xu G, Fromholt D, Gonzales V, Borchelt DR. Environmental enrichment exacerbates amyloid plaque formation in a transgenic mouse model of Alzheimer disease. J Neuropathol Exp

Neurol 2003;62(12):1220-7.

Jin M, Shepardson N, Yang T, Chen G, Walsh D, Selkoe DJ. Soluble amyloid {beta}-protein dimers isolated from Alzheimer cortex directly induce Tau hyperphosphorylation and neuritic degeneration. Proc Natl Acad Sci U S A 2011;108(14):5819-24.

Keller JB, Bevier WC, Jovanovic-Peterson L, Formby B, Durak EP, Peterson CM. Voluntary exercise improves glycemia in non-obese diabetic (NOD) mice. Diabetes Res Clin Pract.1993;22(1):29-35.

Kitaguchi H, Tomimoto H, Ihara M, Shibata M, Uemura K, Kalaria RN, Kihara T, Asada-Utsugi M, Kinoshita A, Takahashi R. Chronic cerebral hypoperfusion accelerates amyloid beta deposition in APPSwInd transgenic mice. Brain Res. 2009; 1294:202-10.

Lambert TJ, Fernandez SM, Frick KM. Different types of environmental enrichment have discrepant effects on spatial memory and synaptophysin levels in female mice. Neurobiol Learn Mem. 2005;83(3):206-16.

Laurin D, Verreault R, Lindsay J, MacPherson K, Rockwood K. Physical activity and risk of cognitive impairment and dementia in elderly persons. Arch Neurol 2001;58(3):498-504

Lazarov O, Robinson J, Tang YP, Hairston IS, Korade-Mirnics Z, Lee VM, Hersh LB, Sapolsky RM, Mirnics K, Sisodia SS. Environmental enrichment reduces Abeta levels and amyloid deposition in transgenic mice. Cell 2005;120(5):701-13.

Lesne S, Koh MT, Kotilinek L, Kayed R, Glabe CG, Yang A, Gallagher M, Ashe KH. A specific amyloid-beta protein assembly in the brain impairs memory. Nature 2006;440(7082):352-7.

Maesako M, Uemura K, Kubota M, Ando K, Kuzuya A, Asada M, Kihara T, Kinoshita A. Insulin regulates Presenilin 1 localization via PI3K/Akt signaling. Neurosci Lett 2010;483(3):157-61.

Maesako M, Uemura K, Kubota M, Hiyoshi K, Ando K, Kuzuya A, Kihara T, Asada M, Akiyama H, Kinoshita A. Effect of glycogen synthase kinase 3 beta-mediated presenilin 1 phosphorylation on amyloid beta production is negatively regulated by insulin receptor cleavage. Neuroscience 2011;177:298-307.

McClean PL, Parthsarathy V, Faivre E, Holscher C. The diabetes drug liraglutide prevents degenerative processes in a mouse model of Alzheimer's disease. J Neurosci 2011;31(17):6587-94.

Misra P. AMP activated protein kinase: a next generation target for total metabolic control. Expert Opin Ther Targets. 2008;12(1):91-100.

Mucke L, Masliah E, Yu GQ, Mallory M, Rockenstein EM, Tatsuno G, Hu K, Kholodenko D, Johnson-Wood K, McConlogue L. High-level neuronal expression of abeta 1-42 in wild-type human amyloid protein precursor transgenic mice: synaptotoxicity without plaque formation. J Neurosci 2000;20(11):4050-8.

Ott A, Stolk RP, van Harskamp F, Pols HA, Hofman A, Breteler MM. Diabetes mellitus and the risk of dementia: The Rotterdam Study. Neurology 1999;53(9):1937-42.

Panza F, Capurso C, D'Introno A, Colacicco AM, Del Parigi A, Seripa D, Pilotto A, Capurso A, Solfrizzi V. Diet, cholesterol metabolism, and Alzheimer's disease: Apolipoprotein E as a possible link? J Am Geriatr Soc 2006;54(12):1963-5.

Pedersen WA, McMillan PJ, Kulstad JJ, Leverenz JB, Craft S, Haynatzki GR. Rosiglitazone attenuates learning and memory deficits in Tg2576 Alzheimer mice. Exp Neurol 2006;199(2):265-73.

Qiu WQ, Folstein MF. Insulin, insulin-degrading enzyme and amyloid-beta peptide in Alzheimer's disease: review and hypothesis. Neurobiol Aging. 2006 Feb;27(2):190-8.

Reger MA, Watson GS, Green PS, Wilkinson CW, Baker LD, Cholerton B, Fishel MA, Plymate SR, Breitner JC, DeGroodt W, Mehta P, Craft S. Intranasal insulin improves cognition and modulates beta-amyloid in early AD. Neurology 2008;70(6):440-8.

Sanz C, Gautier JF, Hanaire H. Physical exercise for the prevention and treatment of type 2 diabetes. Diabetes Metab 2010;36(5):346-51.

Scarmeas N, Luchsinger JA, Mayeux R, Stern Y. Mediterranean diet and Alzheimer disease mortality. Neurology 2007;69(11):1084-93.

Shankar GM, Li S, Mehta TH, Garcia-Munoz A, Shepardson NE, Smith I, Brett FM, Farrell MA, Rowan MJ, Lemere CA, Regan CM, Walsh DM, Sabatini BL, Selkoe DJ. Amyloid-beta protein dimers isolated directly from Alzheimer's brains impair synaptic plasticity and memory. Nat Med 2008;14(8):837-42.

Solfrizzi V, Panza F, Capurso A. The role of diet in cognitive decline. J Neural Transm 2003;110(1):95-110.

Stockley JH, O'Neill C. Understanding BACE1: essential protease for amyloid-beta production in Alzheimer's disease. Cell Mol Life Sci 2008;65(20):3265-89.

Takasugi N, Sasaki T, Suzuki K, Osawa S, Isshiki H, Hori Y, Shimada N, Higo T, Yokoshima S, Fukuyama

T, Lee VM, Trojanowski JQ, Tomita T, Iwatsubo T. BACE1 activity is modulated by cell-associated sphingosine-1-phosphate. J Neurosci 2011;31(18):6850-7.

Takeda S, Sato N, Uchio-Yamada K, Sawada K, Kunieda T, Takeuchi D, Kurinami H, Shinohara M, Rakugi H, Morishita R. Diabetes-accelerated memory dysfunction via cerebrovascular inflammation and Abeta deposition in an Alzheimer mouse model with diabetes. Proc Natl Acad Sci U S A;107(15):7036-41.

Tandon A, Rogaeva E, Mullan M, St George-Hyslop PH. Molecular genetics of Alzheimer's disease: the role of beta-amyloid and the presenilins. Curr Opin Neurol 2000;13(4):377-84.

Walsh DM, Klyubin I, Fadeeva JV, Cullen WK, Anwyl R, Wolfe MS, Rowan MJ, Selkoe DJ. Naturally secreted oligomers of amyloid beta protein potently inhibit hippocampal long-term potentiation in vivo. Nature 2002;416(6880):535-9.

Watson GS, Cholerton BA, Reger MA, Baker LD, Plymate SR, Asthana S, Fishel MA, Kulstad JJ, Green PS, Cook DG, Kahn SE, Keeling ML, Craft S. Preserved cognition in patients with early Alzheimer disease and amnestic mild cognitive impairment during treatment with rosiglitazone: a preliminary study. Am J Geriatr Psychiatry 2005;13(11):950-8.

Xia W, Yang T, Shankar G, Smith IM, Shen Y, Walsh DM, Selkoe DJ. A specific enzyme-linked immunosorbent assay for measuring beta-amyloid protein oligomers in human plasma and brain tissue of patients with Alzheimer disease. Arch Neurol 2009;66(2):190-9.

7. Figure legends

Fig. 1.**Schematic presentation of our experimental design**

APP*Swe/Ind* mice were maintained with standard diet in the standard laboratory cages until 2-3 months age. Then, age- and sex-matched mice were separated into 3 groups. In the control group, the mice were induced with standard diet in the standard laboratory cages for 20 weeks (control APP mice) (top row, n = 9). In the high fat diet (HFD) induced group, the mice were fed with HFD in the standard laboratory cages for 20 weeks (APP-HFD mice) (middle row, n = 10). In the HFD with environmental enrichment (EE) induced group, the mice spent 10 weeks in the standard laboratory cages, then spent 10 weeks in the enrichment cages with HFD (APP-HFD+EE mice) (bottom row, n = 8). After 20 weeks, metabolic

conditions of these mice were analyzed, followed by ethological, histochemical and biochemical analyses targeting AD pathophysiology.

Fig. 2.**Environmental enrichment ameliorated HFD-induced diabetic conditions**

(*A)* Relative body weight changes over 20 weeks. The body weight of 2 weeks before each diet was regarded as the baseline (100 %). The bodyweight of APP-HFD mice was significantly increased compared with that of control APP mice ($F_{(2, 528)} = 136.81$, $p < 0.05$). On the other hand, that of APP-HFD +EE mice was significantly decreased compared with that of APP-HFD mice ($p < 0.05$).

(*B)* Fasting glucose levels. The fasting glucose level of APP-HFD mice was significantly increased compared with that of control APP mice ($F_{(2, 24)} = 19.38$, $p = 0.02$). On the other hand, the fasting glucose level of APP-HFD+EE mice was significantly decreased compared with that of APP-HFD mice ($p = 0.03$).

(C) Blood glucose levels during glucose tolerance test after an intra-peritoneal injection of glucose (2 g/kg body weight). APP-HFD mice showed impaired glucose tolerance compared with control mice ($F_{(2, 72)} = 35.00$, $p < 0.05$). On the other hand, APP-HFD+EE had ameliorated HFD-induced glucose intolerance ($p < 0.05$).

(D) Serum insulin levels during fasting or 60 min after glucose injection. At both time points, the serum insulin level of APP-HFD mice was significantly increased compared with that of control APP mice ($F_{(2, 24)} = 8.08$, $p = 0.003$). The serum insulin level of APP-HFD+EE mice was not significantly decreased compared with that of APP-HFD mice (n.s., $p = 0.27$). n.s. indicated not significantly.

Fig. 3.**Environmental enrichment could not ameliorate HFD-induced lipid dysfunction**

(*A)* Plasma total cholesterol levels. The total cholesterol level of APP-HFD mice was significantly increased compared with that of control APP mice ($F_{(2, 24)} = 24.28$, $p = 0.0003$). That of APP-HFD+EE mice was not significantly decreased compared with that of APP-HFD mice (n.s., $p = 0.14$). n.s. indicated not significantly.

(B) Plasma HDL cholesterol levels. The HDL cholesterol level of APP-HFD mice was significantly increased compared with that of control APP mice ($F_{(2, 24)} = 17.37$, $p = 0.0003$). The HDL cholesterol level of APP-HFD+EE mice was not significantly decreased compared with that of APP-HFD mice (n.s., $p = 0.17$). n.s. indicated not significantly.

(C) Plasma triglyceride levels. There was no difference among control, APP-HFD and APP-HFD+EE mice. ($F_{(2, 24)} = 1.33$, n.s.)

Fig. 4.**Environmental enrichment ameliorated HFD-induced memory deficit**

(A) Escape latency in the acquisition phase. APP-HFD mice significantly took longer time to the platform compared with control APP mice ($F_{(2, 96)} = 17.33$**,** $p = 0.012$). On the other hand, APP-HFD+EE mice took less time than APP-HFD mice ($p = 0.34$).

(*B)* Swimming length in the acquisition phase. APP-HFD mice swam significantly longer than control APP mice ($F_{(2, 96)} = 11.92$**,** $p = 0.025$). On the other hand, APP-HFD+EE mice swam shorter than APP-HFD mice ($p = 0.37$).

(C) The time to the target quadrant in the probe trial phase. APP-HFD mice significantly took longer time to the platform quadrant compared with control APP mice ($F_{(2, 24)} = 33.02$, $p= 0.002$). On the other hand, APP-HFD+EE mice took less time than APP-HFD mice ($p = 0.002$).

(D) The number of entries into the target quadrant in the probe trial phase. APP-HFD mice were significantly impaired in the number of times they crossed the platform compared with control APP mice ($F_{(2, 24)} = 15.75$, $p = 0.0014$). On the other hand, APP-HFD+EE mice increased the number of times they crossed the platform compared with APP-HFD mice ($p = 0.003$).

Fig. 5.**Environmental enrichment ameliorated HFD-induced Aβ accumulation**

(A) Immunohistochemical analysis using anti-Aβ (6E10) antibody. Representative images of Aβ-immunostained hippocampus sections from control APP, APP-HFD and APP-HFD+EE induced mice, respectively. Scale bar, 2 mm

(B) High-magnification images of the hippocampus including CA1 and Dentate Gyrus (DG) regions by immunostained analysis using anti-Aβ (6E10) antibody and Alexa Fluor 488 2^{nd} antibody. The immunostained signal was much enhanced in APP-HFD mice compared with that in control APP and APP-HFD+EE mice. Scale bar, 0.5 mm

(*C)* Cerebral Aβ loads determined by immunohistochemical and morphometric analyses. The cerebral Aβ deposition was significantly increased in APP-HFD mice compared with that in control APP mice ($F_{(2, 10)}$

= 5.62, p = 0.012). On the other hand, that in APP-HFD+EE mice was significantly decreased compared with that in APP-HFD mice (p = 0.023).

(*D*) ELISA of Aβ 40 in TBS-soluble fraction. The level of TBS-soluble Aβ 40 in APP-HFD mice was the same as that in control APP mice. On the other hand, that in APP-HFD+EE was significantly decreased compared with that in APP-HFD mice ($F_{(2, 10)} = 5.16$, p = 0.015).

(*E*) ELISA of Aβ 42 in TBS-soluble fraction. There was no statistical significance among control APP, APP-HFD and APP-HFD+EE induced mice ($F_{(2, 10)} = 1.05$, n.s.).

(*F*) ELISA of total Aβ (Aβ 40 + Aβ 42) in TBS-soluble fraction. The level of TBS-soluble total Aβ in APP-HFD mice was the same as that in control APP mice. On the other hand, that in APP-HFD+EE was significantly decreased compared with that in APP-HFD mice ($F_{(2, 10)} = 6.35$, p = 0.037).

(*G*) ELISA of Aβ oligomer in TBS-soluble fraction. The cerebral Aβ oligomer was significantly increased in APP-HFD mice compared with that in control APP mice ($F_{(2, 10)} = 5.19$, p = 0.01). On the other hand, that in APP-HFD+EE was significantly decreased compared with that in APP-HFD mice (p= 0.049).

Fig. 6.**Environmental enrichment reduced APP CTFβ accumulation**

(A) Immunoblotting analysis of APP full length, APP CTFs (CTFα, β) and APP CTFβ. APP full length and APP CTFs were detected by anti-APP c-terminus antibody. APP CTFβ was detected by anti-Aβ (6E10) antibody. Two different samples from each group were shown. β-actin was detected as loading control.

(B) Statistical analysis of APP full length. The band of APP full length was normalized by that of β-actin. The band density of the control was regarded as 100 % and that of other groups was relatively indicated. There was no statistical significance among control APP, APP-HFD and APP-HFD+EE mice ($F_{(2, 10)} = 2.36$, n.s.).

(C) Statistical analysis of APP CTFs. The band of APP CTFs was normalized by that of APP full length. The band density of APP CTFs in APP-HFD mice was increased compared with that in control APP mice ($F_{(2, 10)} = 4.73$, p = 0.013). On the other hand, that in APP-HFD+EE mice was significantly decreased compared with that in APP-HFD mice (p = 0.015).

(D) Statistical analysis of APP CTFβ. The band of APP CTFβ was normalized by that of APP full length. The band density of APP CTFβ in APP-HFD mice was increased compared with that in control APP mice

($F_{(2, 10)} = 5.67$, $p = 0.011$). On the other hand, that in APP-HFD+EE mice was significantly decreased compared with that in APP-HFD mice ($p = 0.032$).

Maesako et al. Fig. 1

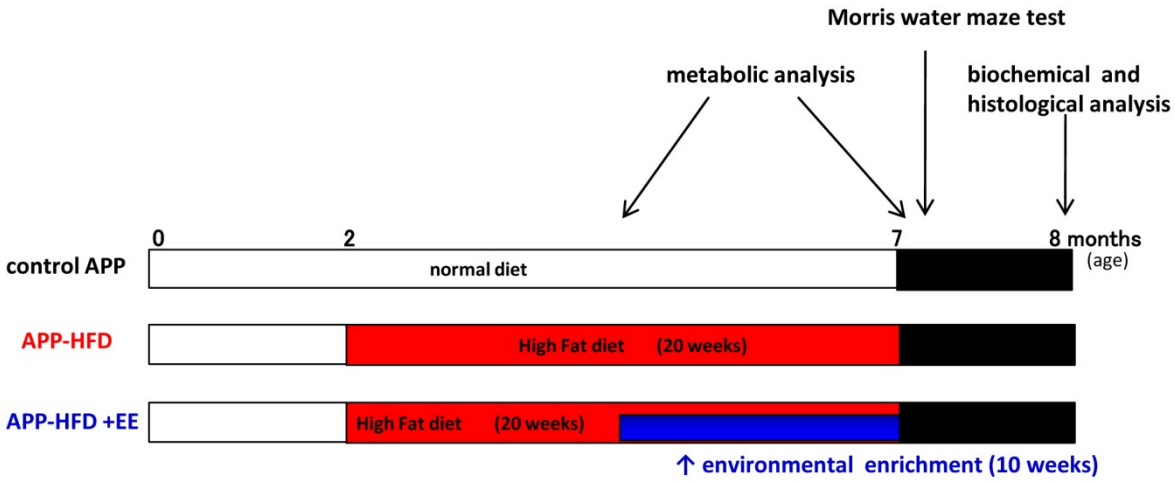

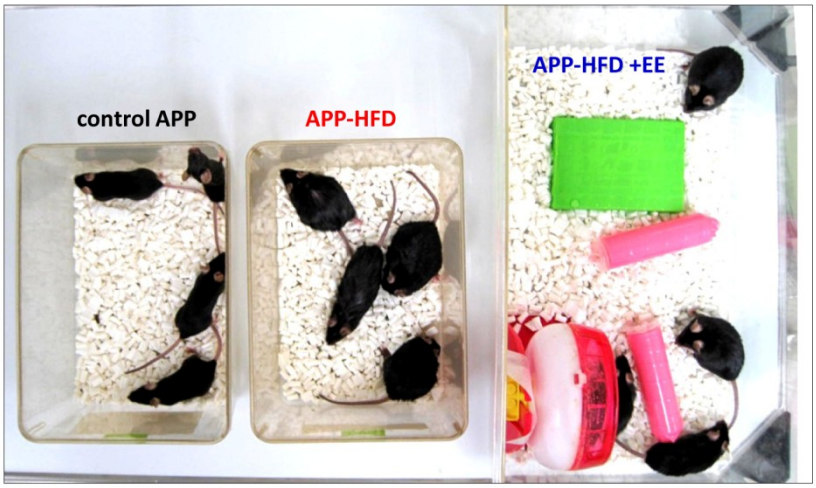

Maesako et al. Fig. 2

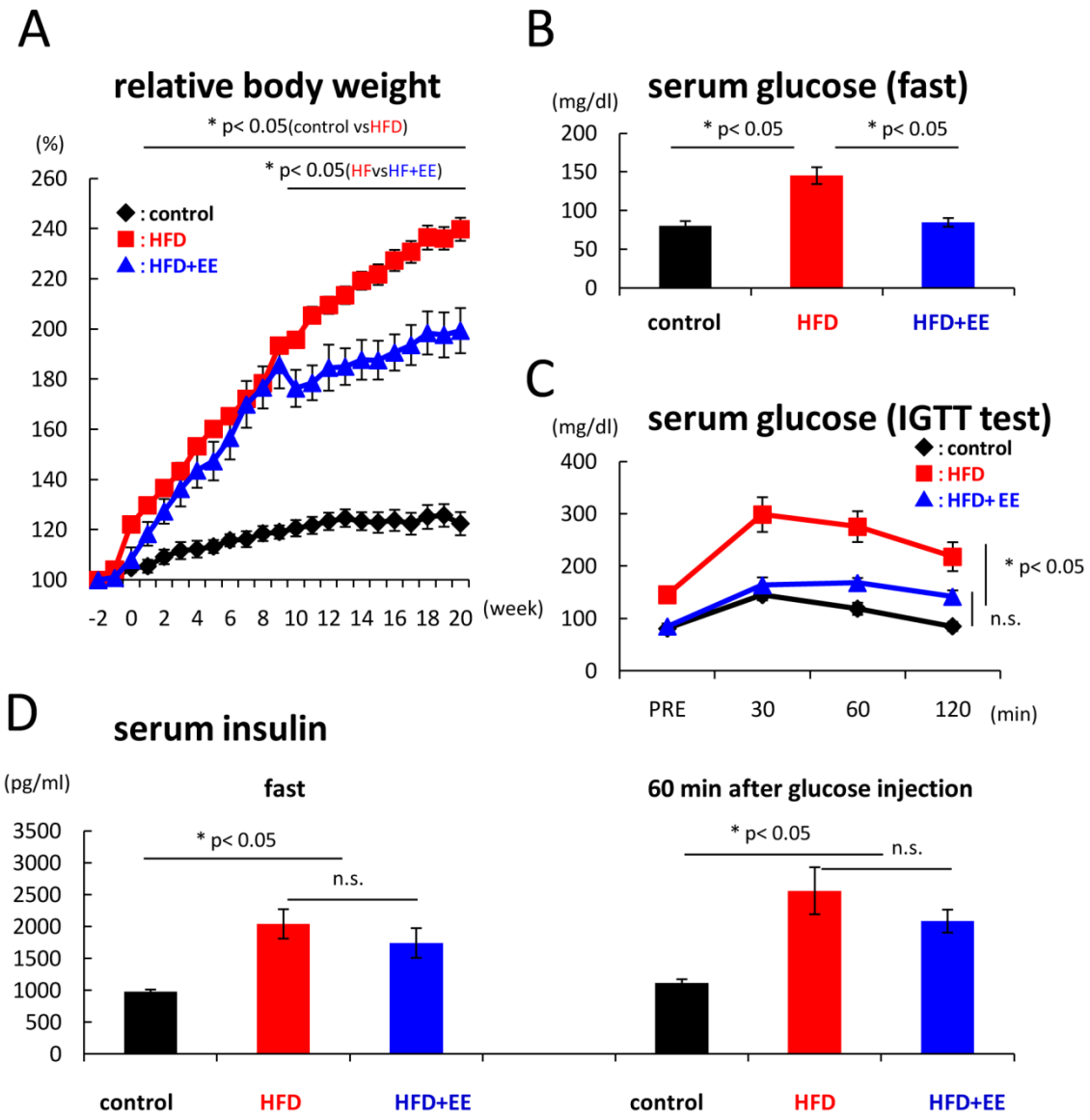

Maesako et al. Fig. 3

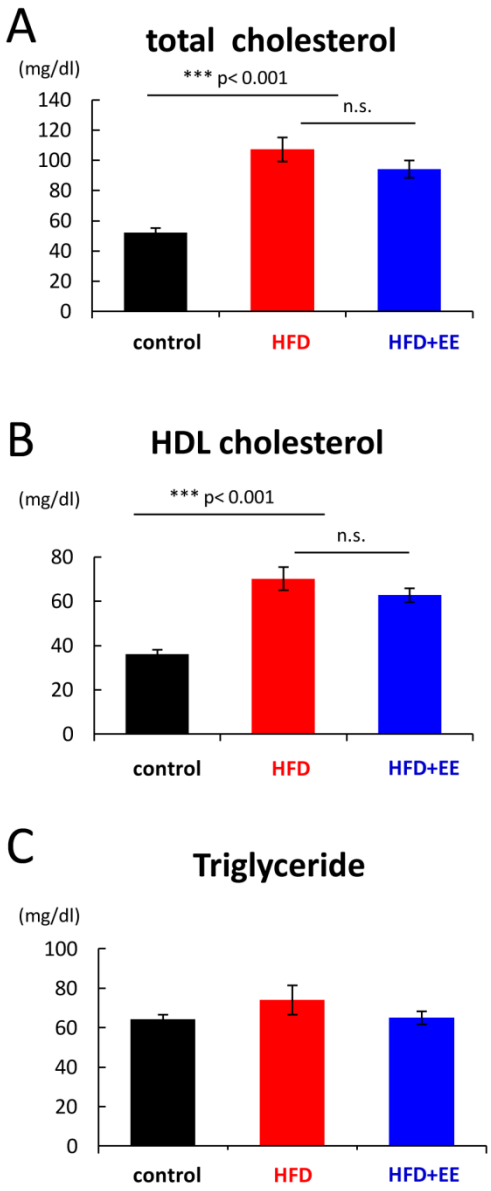

Maesako et al. Fig. 4

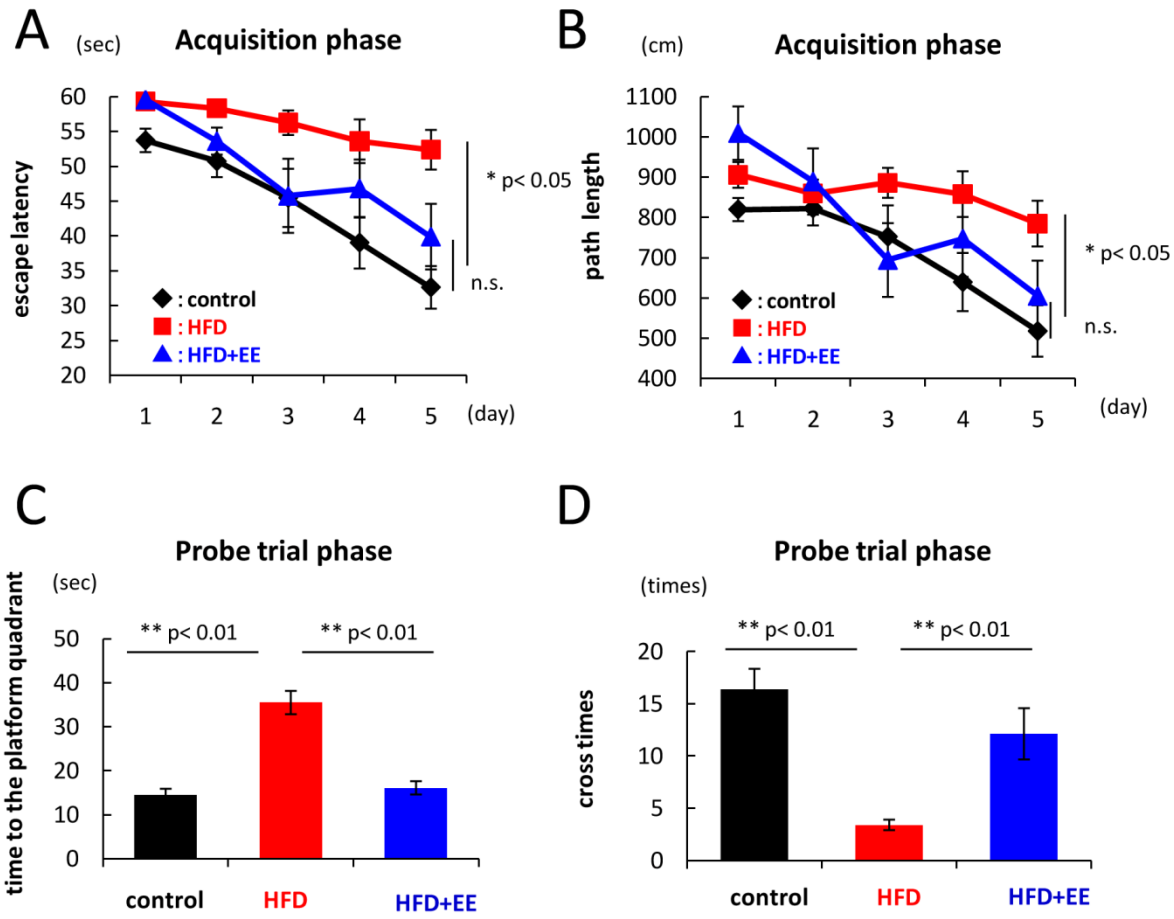

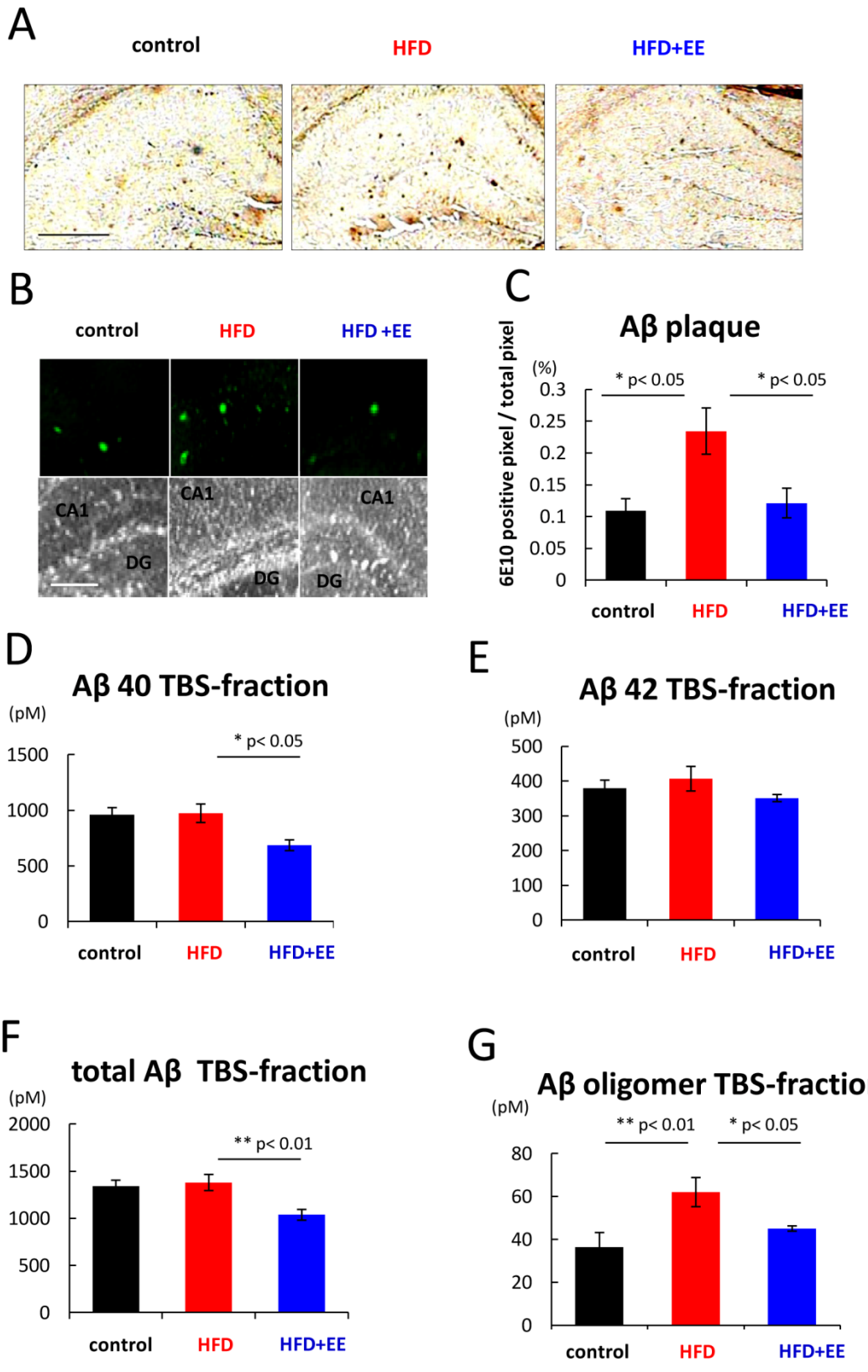
A
control
HFD
HFD+EE
B
control
HFD
HFD +EE
CA1
DG
C
Aβ plaque
6E10 positive pixel / total pixel
(%)
* p< 0.05
* p< 0.05
control
HFD
HFD+EE
D
Aβ 40 TBS-fraction
(pM)
* p< 0.05
E
Aβ 42 TBS-fraction
(pM)
F
total Aβ TBS-fraction
(pM)
** p< 0.01
G
Aβ oligomer TBS-fraction
(pM)
** p< 0.01
* p< 0.05

Maesako et al. Fig. 6